Construction and Building Materials 319 (2022) 126064

Contents lists available at ScienceDirect

Construction and Building Materials

journal homepage: www.elsevier.com/locate/conbuildmat

All-lignocellulosic fiberboards from giant reed (*Arundo donax* L.): Effect of steam explosion pre-treatment on physical and mechanical properties

Federica Vitrone [a,*], Diego Ramos [b], Vittoria Vitagliano [b], Francesc Ferrando [b], Joan Salvadó [a]

[a] Rovira i Virgili University, Department of Chemical Engineering, Avinguda dels Països Catalans, 26 43007 Tarragona, Catalonia, Spain
[b] Rovira i Virgili University, Department of Mechanical Engineering, Avinguda dels Països Catalans, 26, 43007 Tarragona, Catalonia, Spain

ARTICLE INFO

Keywords:
Binderless Fiberboards
Arundo donax L.
Steam Explosion
Severity Factor
Sustainability

ABSTRACT

Steam explosion has proved to be one of the treatments which produces the best physical and mechanical results in the production of fiberboards without adding adhesives. Perhaps the main drawback is energy consumption, making process optimization essential. The aim of this study was to explore the effect of five severity (R_0) levels of steam explosion pre-treatment on mechanical and physical properties of binderless fiberboards, made with giant reed (*Arundo donax* L.). Results showed that fiberboard properties significantly improve within a 5 °C range of pre-treatment temperature (Tr) and then get worse after exceeding the maximum Tr of 200 °C. Therefore, the best results were obtained for the 200 °C Tr and the average values were MOR 4538,50 N/mm^2, MOE 34.67 N/mm^2, IB 4.079 N/mm^2, TS 7.50%, and WA 9.13%. Scanning electron microscope (SEM) observation and Fourier-transform infrared (FT-IR) spectra analysis confirmed that major morphological and chemical changes occurred in the Tr range of 190–195 °C. Finally, by means of Thermogravimetric analysis (TGA), the limiting oxygen index (LOI) was calculated to derive information regarding the material's ability to be both flame retardant and self-extinguishing.

1. Introduction

The building sector has always made an extensive use of forest resources to produce wood-based panels like particleboards, plywood, strand boards, and fiberboards [1]. Fiberboards are prefabricated components made of lignocellulosic fibers, which can be used in the construction of furniture, insulation, soundproofing, and other functions [2]. Sala et al. [3] reported that the fabrication of fiberboards in Europe has increased from 8.4 to 18 Mm^3 between 2000 and 2018. Moreover, the building sector is moving increasingly towards prefabrication and fiberboards are well suited for this use, both for the domestic building sector and the construction of industrial buildings [4]. This consequently requires the timber industry to produce more wood products to meet the market demand. However, the high market demand results in the overexploitation of natural resources and an increase in the rate of deforestation [1,5]. According to the European "EUwood" study, the deficit of wood is expected to be 300 million m^3 by 2030 [6].

On the other hand, the threats to health and the environment, due to the use of formaldehyde-based adhesives to bond the fibers, must be considered [7]. In fact, formaldehyde-based adhesives are non-biodegradable and contain non-recyclable constituents [4,8]. During their production and service life they can pollute the environment because of the formaldehyde emissions, in addition to being hazardous for end users [9].

For all these reasons, research in the field of fiberboard production focuses on two main challenges: (i) to find alternative materials that can meet the high demand without compromising the stability of the ecosystem and (ii) to produce binder-free or completely bio-based fiberboards with the dual purpose of stopping formaldehyde emissions and giving more opportunities for recycling fiberboards at their end of life.

In considering these issues, research has focused on using agricultural or industrial by-products to solve the overexploitation of natural resources. Annual plant stem provides suitable, renewable, and safer alternative raw materials [1]. In addition, the need to repair the health and environmental consequences generated by the emissions of

Abbreviations: MOE, Modulus of elasticity; MOR, Modulus of rupture; IB, Internal bond; TS, thickness swelling; WA, water absorption; IB, internal bond; Tr, pre-treatment (steam explosion) temperature; tr, pre-treatment (steam explosion) retention time; R_0, pre-treatment (steam explosion) severity; Tp, pressing temperature; Pp, press pressure; tp, pressing time; Tc, curing (final heat treatment) temperature; tc, curing (final heat treatment) time.

* Corresponding author.
E-mail address: federica.vitrone@urv.cat (F. Vitrone).

https://doi.org/10.1016/j.conbuildmat.2021.126064
Received 31 July 2021; Received in revised form 2 December 2021; Accepted 7 December 2021
Available online 16 December 2021

Table 1
Chemical characterization of *Arundo donax* L. raw material and *Arundo donax* L. pulp.

Raw material	Hemicellulose (%)	Cellulose (%)	Lignin (%)	Ash-C (%)	Extract (%)	Reference
Arundo donax	14,5–32	29,2–43.1	19,2–24,3	4,2–6,1	9.3	[25,26,42,50]
Arundo donax pulp	5.2 ± 0.8	55.4 ± 0.9	29 ± 0.9	1.2 ± 0.2	5.9 ± 0.5	[42]

Fig. 1. Photo of the cylindrical reactor and the expansion chamber.

formaldehyde-based adhesives led researchers to look for the most suitable treatments which can activate a bonding ability of lignin, in order to fabricate binderless fiberboards [2].

Some of the non-conventional raw materials that have been recently employed in binderless fiberboard manufacturing are: grapevine waste [10], wheat and rapeseed straw [11], coconut husks [12], coriander [13], rattan fibers [14], macadamia shells [15], bagasse [16], totora [17], wheat straw [4,18,19], rice straw [20,21], almond residues [22], hemp fibers and rice husks [23], and corn stalk [24].

Perennial grasses, such as *Arundo donax* L., also represent a viable alternative in the search for suitable alternative raw materials for fiberboard production, as they are generally widespread and can grow spontaneously in different kinds of environments [25,26]. *Arundo donax* L., commonly known as giant reed, is considered a multipurpose crop [27]. Chemical compounds of *Arundo donax* L. raw material and *Arundo donax* L. pulp are reported in Table 1. Its features are that it is fast-growing, adaptable to different climatic conditions, and has low input requirements [28]. Angelini et al. [29] studied the biomass yield and the energy balance of *Arundo donax* L, by considering different management practices. They found a ratio of energy output and energy input which was very favorable between the 1st and the 6th year of cultivation, and a high yield also confirmed in other studies [30]. Jambor et al [31] published an in-depth bibliographic study confirming a very high energy balance of *Arundo donax* L. Moreover, in this work some studies reported registering that a high initial investment was needed for *Arundo donax* L. cultivation, but also incurring very low maintenance costs, which repay the expense in the long term [31]. Furthermore, F. W. Croon [32] in his work studied how the use of reeds can be a favourable source for pulp production, thermal energy, second generation bioethanol production, and the production of fiberboards. In all cases the use of reeds can be economically favorable, considering that their cultivation does not need complex infrastructures and does not compete with food crops. Giant reed is also considered one of the world's 100 most invasive species and it has been included in the Spanish Catalogue of Invasive Species [33]. Due to its vegetative reproduction, it easily occupies new areas by forming dense masses, thus causing the alteration of the ecosystem, and affecting the growth of native species [33,34].

This situation prompted attempts to take advantage of giant reed by using it for biogas production [35,36], papermaking [37], extraction of chemical compounds [25], musical instruments [38], and phytoremediation of contaminated soils [39].

Recently, giant reed has also become popular in the production of particleboards and fiberboards [40-42]. *Arundo donax* L. has already been used as a structural material in traditional architecture [32]. Molari et al. [43], studied mechanical properties of giant reeds starting from their traditional structural use. They found a similar behavior to various species of bamboo used in construction and thus they showed the potential of using giant reed as construction structural material.

Nonetheless, to our knowledge, research in the field of binderless fiberboards made by giant reed is still limited. For instance, Ferrandez-Villena et al. [33] evaluated mechanical and physical properties of binderless fiberboards made by giant reed rhizome, achieving a modulus of rupture (MOR) of 14.2 N/mm^2, a modulus of elasticity (MOE) of 2052.45 N/mm^2, and an internal bonding strength (IB) of 1.12 N/mm^2. Ferrandez-Garcia et al. [44] developed an eco-friendly board from giant reed and citric acid as a natural binder, proving its suitability as insulating material, since it has a thermal conductivity ranging between 0.081 and 0.093 W/m K. Some studies [41,42] explored the steam explosion pre-treatment of *Arundo donax* L. for binderless fiberboard production. In these studies, the steam explosion pre-treatment led to high quality boards, having an MOE of 7439 N/mm^2, an MOR of 40.4 N/mm^2, an IB of 1.28 N/mm^2, a water absorption (WA) of 17.6%, and a thickness swelling (TS) of 13.3%. This showed the feasibility of *Arundo donax* L. as raw material for binderless fiberboard manufacture, provided that pre-treatment is carried out.

Among pre-treatments of lignocellulosic materials, steam explosion pre-treatment has been claimed to be particularly successful [2,45]. This results in the separation of lignocellulosic materials into their major components [45], via high pressure steam and sudden decompression. This process is known as "Masonite process" [46], which by applying high temperature and high steam pressure, enables the processing of lignocellulosic fibers in order to obtain the hemicellulose degradation and the lignin softening [47]. This permits the redistribution of lignin onto the cellulose surface [8], thus enhancing the self-bonding of the fibers and the improvement of dimensional stability [2]. Previous research studied the employment of steam explosion pre-treatment in the production of binderless fiberboards and the effect of pre-treatment temperature (Tr) and retention time (tr) on the properties of the boards. For example, Kurokochi et al. [48] studied the effect of steam explosion

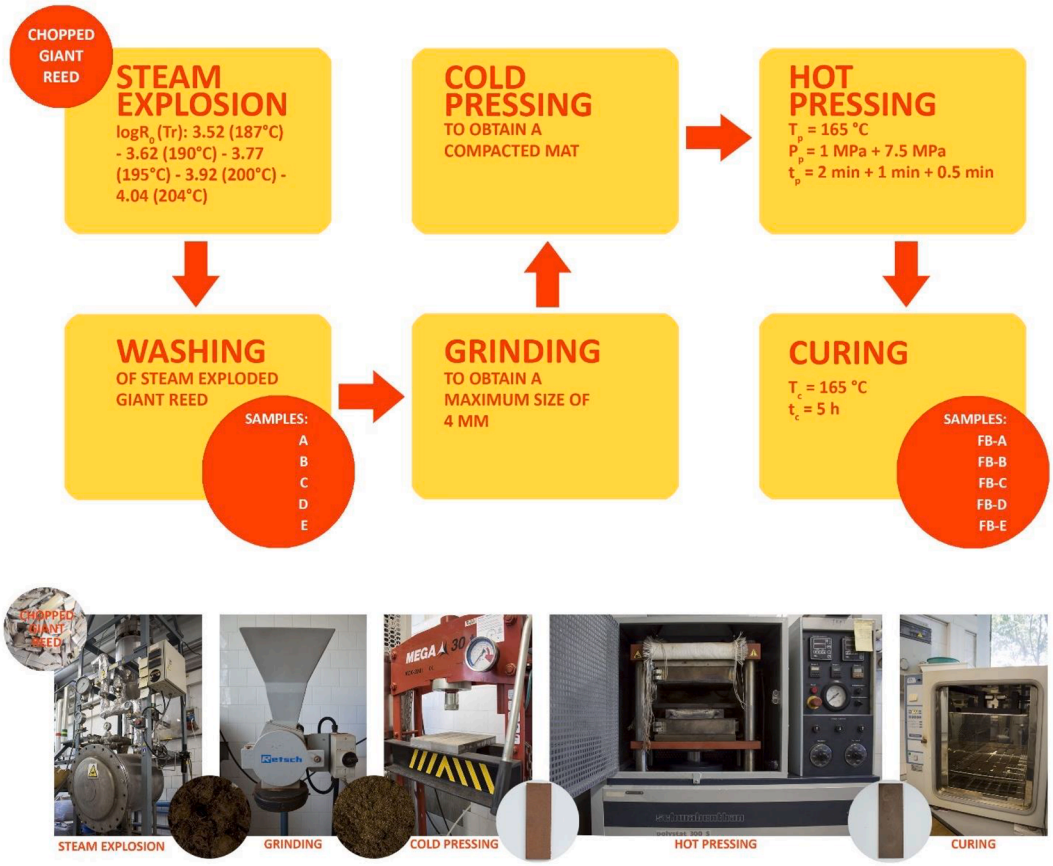

Fig. 2. Flowchart and photos of the manufacturing process of binderless fiberboards made by *Arundo donax* L.

Table 2
Summary of some minimum values for boards properties from standard regulation UNE-EN 312:2010.

		Thickness	MOE	MOR	IB	TS
Nomenclature	Usage	mm	N/mm^2	N/mm^2	N/mm^2	%
P1	General use in dry conditions	3–6	–	11.5	0.31	–
P6	High performance structural use in dry conditions	3–4	2800	18	0.65	18
P7	High performance structural use in wet conditions	3–4	3000	20	0.75	10

pre-treatment carried out at 200 °C for 10 or 20 min, on rice straw binderless fiberboards. They obtained a great improvement in IB, and TS justified by the hemicellulose and cellulose decomposition, and also the lignin degradation which occurs during steam treatment. Mejía et al [8] compared mechanical and physical results of binderless fiberboards made by oil palm waste treated by steam explosion and oxidated by Fenton's reagent. Their study showed that the high performance of binderless boards can be achieved by steam explosion pre-treatment carried out at a severity factor ($logR_0$) of 4.0, which led to optimum values of MOE 3100 N/mm^2, MOR 28.49 N/mm^2, TS 11.80%, and WA 22.74%. Luo et al. [47] studied the effect of increasing tr from 60 to 180 s, with a steam pressure of 3.0 MPa, in binderless fiberboard properties made by bamboo processing residues. The increasing in tr produced an improvement in all mechanical and physical properties and they were able to obtain panels with a maximum value of 15.9 N/mm^2 for MOR, 0.48 N/mm^2 for IB, and 12% for TS. Quintana et al [49] studied the effect of steam explosion pre-treatment on the physico-mechanical responses of binderless fiberboards made by banana bunches, as well as the effect of pressure conditions. They found the optimum values with a $logR_0$ of 3.55, a pressing temperature (Tp) of 200 °C, and a pressing pressure (Pp) of 14 MPa.

The high consumption of energy may be the main drawback when carrying out steam explosion pre-treatment [2]. For this reason, it may be necessary to define a limit of R_0, beyond which there is no further improvement in terms of physico-mechanical properties of binderless fiberboards.

Thus, this study explored the effect of various R_0 of steam explosion pre-treatment carried out on *Arundo donax* L. fibers with the aim of finding the optimum value beyond which higher R_0 only results in wasted energy as it does not lead to significant improvement in material and fiberboard properties. To achieve the objective, we compared the effect of different R_0 on physical and mechanical properties of binderless fiberboards, and we related them to chemical changes mainly due to the steam explosion pre-treatment and the R_0.

2. Materials and methods

2.1. Material and specimen fabrication

The *Arundo donax* L. reeds used in this study were kindly provided by Cañizos Albatera SI and came from Ribarroja de Turia, Valencia (Spain). After manually removing all the leaves attached to the stems, the stems were shredded with Gartenhäcksler Modell LH 280 A (Ahien, Germany)

Table 3
Mean values of physico-mechanical properties, standard deviation, standard error, and possible usage according to European Standard (UNE-EN 312:2010) of binderless fiberboards made by steam exploded giant reed.

Board Type	Tr (°C)	N° Sample	Property	Mean value	Standard deviation	Standard error	Usage
FB-A	187	11	Density (kg/m^3)	916.54	25.25	7.61	None
			MOE (N/mm^2)	830.91	210.72	63.54	
			MOR (N/mm^2)	4.18	1.05	0.32	
			IB (N/mm^2)	0.409	0.19	0.06	
			TS (%)	40.48	10.32	3.11	
			WA (%)	67.31	15.21	4.59	
FB-B	190	9	Density (kg/m^3)	923.42	17.86	5.95	None
			MOE (N/mm^2)	1022.44	258.64	86.21	
			MOR (N/mm^2)	4.42	0.90	0.30	
			IB (N/mm^2)	0.631	0.15	0.05	
			TS (%)	38.20	6.81	2.27	
			WA (%)	64.98	13.60	4.53	
FB-C	195	9	Density (kg/m^3)	1054.59	34.20	11.40	P1 - P6
			MOE (N/mm^2)	4292.33	519.27	173.09	
			MOR (N/mm^2)	31.11	3.60	1.20	
			IB (N/mm^2)	2.33	0.40	0.13	
			TS (%)	12.06	1.17	0.39	
			WA (%)	14.97	1.47	0.49	
FB-D	200	10	Density (kg/m^3)	1091.21	29.31	9.27	P1 - P7
			MOE (N/mm^2)	4538.50	219.98	69.57	
			MOR (N/mm^2)	34.67	3.20	1.01	
			IB (N/mm^2)	4.079	0.49	0.15	
			TS (%)	7.50	0.98	0.31	
			WA (%)	9.13	1.06	0.33	
FB-E	204	9	Density (kg/m^3)	1079.06	14.82	4.94	P1 - P6
			MOE (N/mm^2)	4393.44	313.70	104.57	
			MOR (N/mm^2)	31.80	3.79	1.26	
			IB (N/mm^2)	2.861	0.49	0.16	
			TS (%)	11.14	1.30	0.43	
			WA (%)	12.67	1.13	0.38	

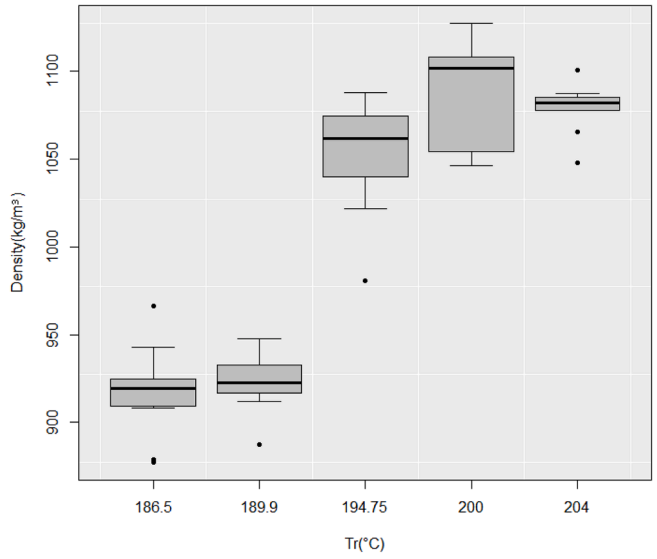

Fig. 3. Boxplots of Density of binderless fiberboards made from steam exploded Arundo donax L at different pre-treatment temperatures (Tr).

to reduce them into chips shorter than 5 mm in length before being pre-treated by steam explosion.

Steam explosion equipment consisted of a 16 L cylindrical reactor at the top and a 100 L expansion chamber at the bottom, connected by a valve, by which the sudden expansion occurs (Fig. 1). About 750 g of chopped reeds were introduced into the batch reactor for each explosion performed. Here the fibers were immersed in saturated steam provided by a Borealis boiler (Vienna, Austria) of 380 V/82 KW at 4 MPa. After a tr of 9.5 min at the required temperatures, the supplied valve was opened and the steam pressure released, causing the disruption of fibers. Several successive explosions were carried out and the material coming from each explosion at the same severity was mixed to obtain a higher homogeneity.

The R_0, which relates Tr and tr, was calculated as follows: [51]

Table 4
ANOVA of the results of the physical and mechanical tests for binderless fiberboards (FB) with respect to treatment severity.

Factor	Property	d. f.	Sum of squares	Mean squares	F	p-value
Tr	Density (kg/m^3)	4	292,562	73,140	112.3	$<2\cdot10^{-16}$
	MOE (MPa)	4	148,478,781	37,119,695	383.8	$<2\cdot10^{-16}$
	MOR (MPa)	4	9715	2428.7	334	$<2\cdot10^{-16}$
	IB (MPa)	4	101.67	25.42	182.2	$<2\cdot10^{-16}$
	TS (%)	4	10,372	2592.9	72.34	$<2\cdot10^{-16}$
	WA (%)	4	35,971	8993	107.2	$<2\cdot10^{-16}$

Table 5
P-value of multiple comparison of physical and mechanical results for binderless fiberboards (FB) by LSD post-hoc test.

FB	Density	MOE	MOR	IB	TS	WA
B-A	0.5813	0.1800	0.8416	0.1940	0.4000	0.5700
C-A	$2\cdot10^{-16}$	$2\cdot10^{-16}$	$2\cdot10^{-16}$	$9\cdot10^{-15}$	$5\cdot10^{-15}$	$2\cdot10^{-16}$
D-A	$2\cdot10^{-16}$	$2\cdot10^{-16}$	$2\cdot10^{-16}$	$2\cdot10^{-16}$	$2\cdot10^{-16}$	$2\cdot10^{-16}$
E-A	$2\cdot10^{-16}$	$2\cdot10^{-16}$	$2\cdot10^{-16}$	$2.1\cdot10^{-12}$	$2\cdot10^{-14}$	$2\cdot10^{-16}$
C-B	$7\cdot10^{-15}$	$2\cdot10^{-16}$	$2\cdot10^{-16}$	$2\cdot10^{-16}$	$4\cdot10^{-13}$	$4\cdot10^{-16}$
D-B	$2\cdot10^{-15}$	$2\cdot10^{-16}$	$2\cdot10^{-16}$	$2\cdot10^{-16}$	$2\cdot10^{-14}$	$2\cdot10^{-16}$
E-B	$2\cdot10^{-16}$	$2\cdot10^{-16}$	$2\cdot10^{-16}$	$3\cdot10^{-16}$	$2\cdot10^{-12}$	$7\cdot10^{-16}$
D-C	0.0028	0.1300	0.0031	$8\cdot10^{-14}$	0.3000	0.2100
E-C	0.0308	0.5600	0.4698	0.004	0.9300	0.7100
E-D	0.4430	0.3900	0.0305	$2\cdot10^{-9}$	0.3700	0.4100

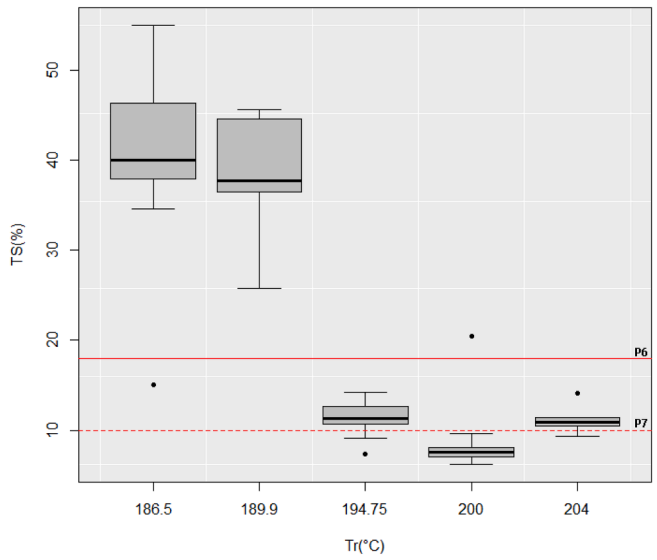

Fig. 4a. Boxplots of Thickness swelling (TS) of binderless fiberboards made from steam exploded Arundo donax L at different pre-treatment temperatures (Tr) and the European standards UNE-EN 312:2010 (P6 and P7 limit values).

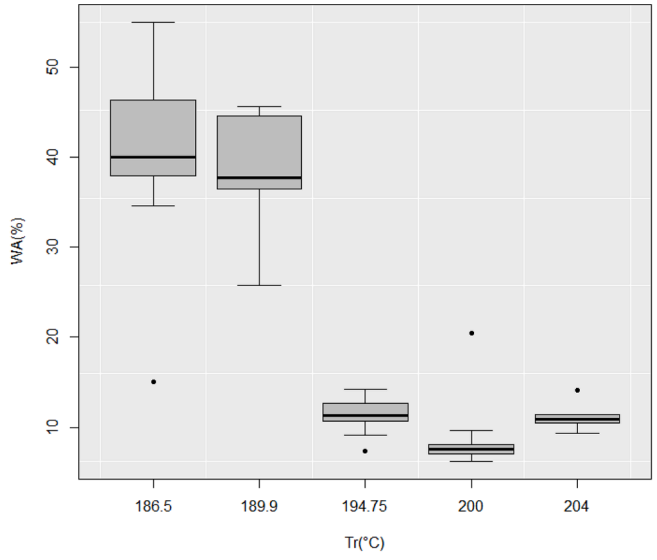

Fig. 4b. Boxplots of Water absorption (WA) of binderless fiberboards made from steam exploded *Arundo donax* L at different pre-treatment temperatures (Tr).

$$R_0 = \int_0^{tr(\min)} \exp[\frac{Tr(C) - 100}{14.75}]dt$$

Five levels of R_0 were used in this study by changing Tr, while tr was kept constant. From our previous studies, we found that a minimum tr of 9.5 min is necessary to let the steam penetrate the fibers, thus enhancing their defibrillation. Therefore, in this study, change in R_0 means change in Tr. The Tr used were 187 °C, 190 °C, 195 °C, 200 °C, 204 °C (which correspond to a logR_0 of 3.52, 3.62, 3.77, 3.92, 4.04 respectively), named A, B, C, D, E respectively.

The exploded *Arundo donax* L. was then rinsed in a washing trolley equipped with a 170 mesh sieve to remove the hydrolyzed hemicellulose. After being left to dry in ambient conditions for about 3 weeks, the exploded *Arundo donax* L. was ground with a Retsch SM 100 mill (Düsseldorf, Germany) equipped with a 4 mm sieve.

About 28.5 g of ground *Arundo donax* L. was cold pressed in a conventional press (MEGA-30 AN, Berriz, Spain) to form a mat of 150x50 mm and approximately 3 mm thickness. The formed mat was conditioned at 20 °C and 65% relative humidity (RH), and then hot pressed in a heated press (Servitec Poystat 300 S, Wustermark, Germany) at Tp 205 °C by a three-step procedure:

- Hot pressing at 1 MPa for 2 min
- Breathing time of 1 min
- Hot pressing at 7.5 MPa for 30 s

Finally, the obtained samples were cured by a final heat treatment carried out in a SELECTA aerated stove of 1600 W, JP Selecta SA (Abrera, Barcelona) at a temperature (Tc) of 165 °C for 5 h, and then conditioned at 20 °C and 65% RH up to constant mass before being tested. The obtained binderless fiberboards were called FB-A, FB-B, FB-

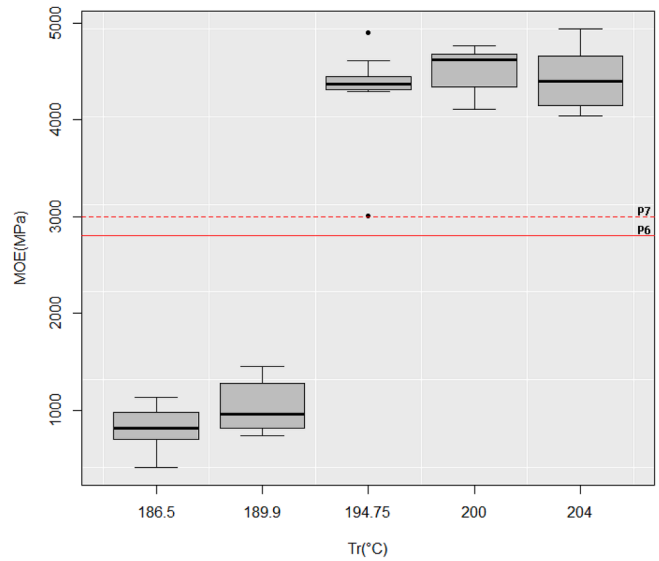

Fig. 5. Boxplots of Modulus of Elasticity (MOE) of binderless fiberboards made from steam exploded Arundo donax L at different pre-treatment temperatures (Tr) and the European standards UNE-EN 312:2010 (P6 and P7 limit values).

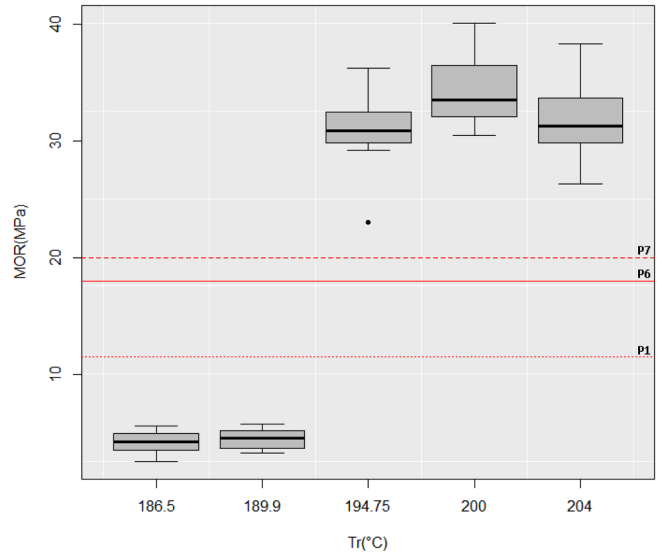

Fig. 6. Boxplots of Modulus of Rupture (MOR) of binderless fiberboards made from steam exploded *Arundo donax* L at different pre-treatment temperatures (Tr) and the European standards UNE-EN 312:2010 (P1, P6, and P7 limit values).

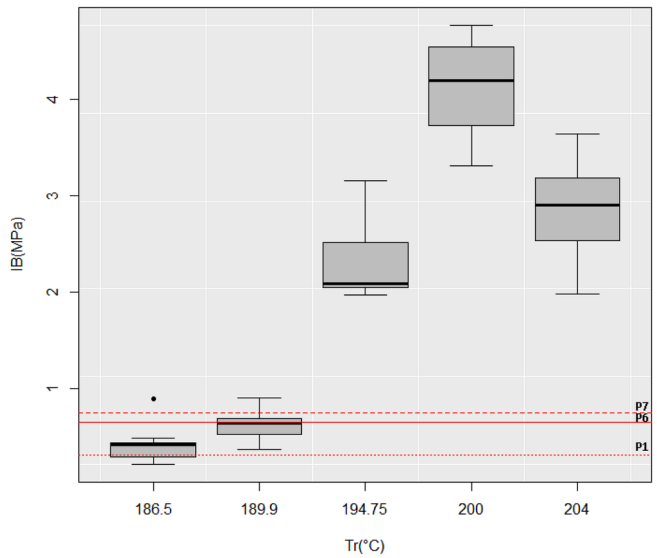

Fig. 7. Boxplots of Internal bonding strength (IB) of binderless fiberboards made from steam exploded Arundo donax L at different pre-treatment temperatures (Tr) and the European standards UNE-EN 312:2010 (P1, P6, and P7 limit values).

C, FB-D, FB-E.

The manufacturing process of binderless fiberboards and the steaming, pressing, and curing conditions are summarized in Fig. 2.

2.2. Measurement of physico-mechanical properties

The European Standards method was followed in order to characterize the specimens. Prior to conduct any mechanical and physical test, the specimens were conditioned in a climatic chamber at 20 °C and 65% RH until constant mass. MOE and MOR were measured according to UNE-EN 310:1994, while IB was calculated following UNE-EN 319:1994. Density and TS were measured in accordance with UNE-EN 323:1993 and UNE-EN 319:1994 respectively. MOR, MOE, and IB test was carried out by using the universal testing machine HOUNSFIELD H10KS. TS and WA were calculated simultaneously by immerging 50x50 mm specimens in a deionized water bath. The specimens were weighed and measured before and after a 24 h period of the water bath, and TS and WA were calculated as thickness and weight difference respectively.

2.3. Statistical analysis

Statistical analysis of physico-mechanical properties was performed by Rstudio software. One-way Analysis of Variance (ANOVA) was used as a statistical method to evaluate the significance of pre-treatment conditions, and Least Significance Difference (LSD) post-hoc test was used to evaluate the difference between the five levels of R_0 considered in this study. A p-value lower than 0.05 was considered as the minimum for the rejection of the null hypothesis.

2.4. Observation by scanning electron microscopy (SEM)

The raw material, the pre-treated fibers and the samples obtained from the break surface of IB test were observed by SEM (FEI ESEM Quanta 600). The samples were mounted on a stub and introduced into the machine to be observed in low vacuum mode. The observation conditions were at acceleration voltages of 15 kV and a distance of approx. 20 mm. All the observations were made at the same magnification of x250 so that different samples could be compared. Prior to observing the pre-treated fibers by SEM, they were dried in the aerated stove at 60 °C for 2 days.

2.5. Fourier-transform infrared (FT-IR) spectra analysis

Infrared spectra of untreated *Arundo donax* L., steam exploded chips, hot pressed and cured fiberboards were obtained to evaluate possible changes in chemical bonds after each treatment. FT-IR 6700 Jasco spectrometer was used. All spectra were collected in the wavenumber range of 4000–400 cm^{-1} with 4 cm^{-1} resolution, and 32 scans for each of the samples.

2.6. Thermogravimetric curves analysis (TGA)

TGA was carried out to determine changes in weight of raw material, and of fiberboards made by exploded fibers, when subjected to a steadily increasing temperature. The TGA was carried out by means of a Mettler TGA/SDTA 851e thermobalance (Columbus, OH, USA). Approx. 10 mg of material was heated at a heating rate of 10 °C/min from 30 °C to 800 °C, under nitrogen atmosphere with a gas flow of 50 mL/min.

3. Results and discussion

3.1. Physical and mechanical results of binderless fiberboards

The mean values of physico-mechanical properties obtained are reported in Table 3

Referring to the standard regulation UNE-EN 312:2010, of which some minimum values are summarized in Table 2, the results obtained (Table 3) can be divided into two groups delimited by the Tr of 195 °C. Beneath the Tr of 195 °C, the obtained binderless fiberboards did not fulfill the requirements even for general use in dry conditions (P1), while above the Tr of 195 °C the requirements were fulfilled, up to high performance structural use in dry conditions (P6). On the other hand, the high performance structural use in wet conditions (P7) need a maximum TS of 10%, and this requirement was not always met. The results which allow this latter usage only belonged to pre-treatment D, i.e. at Tr 200 °C. Commercial fiberboards normally have a MOE ranging between 2670 and 4299 MPa, a MOR of 41.70–42.25 MPa, an IB of 0.39–0.47 MPa, and a TS ranging between 13 and 66% [52], and the results

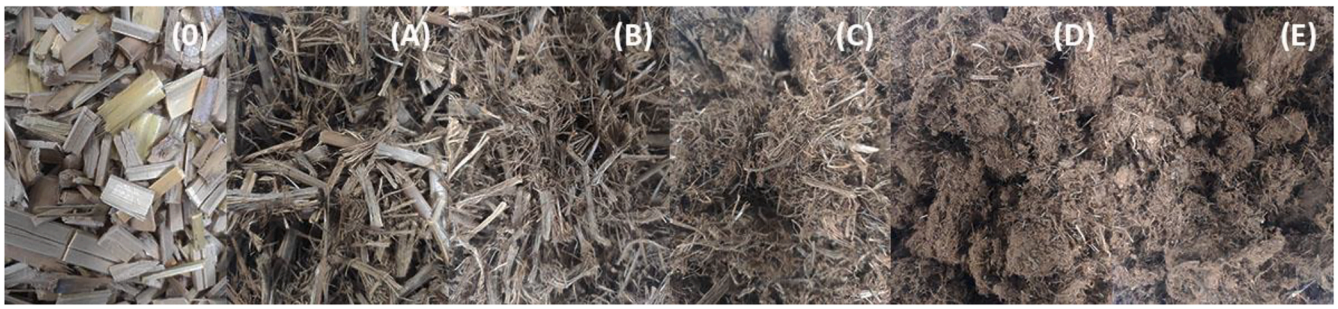

Fig. 8. Photos of raw material (0) and steam exploded Arundo donax L. at Tr 187 °C (A), 190 °C (B), 195 °C (C), 200 °C (D), and 204 °C (E).

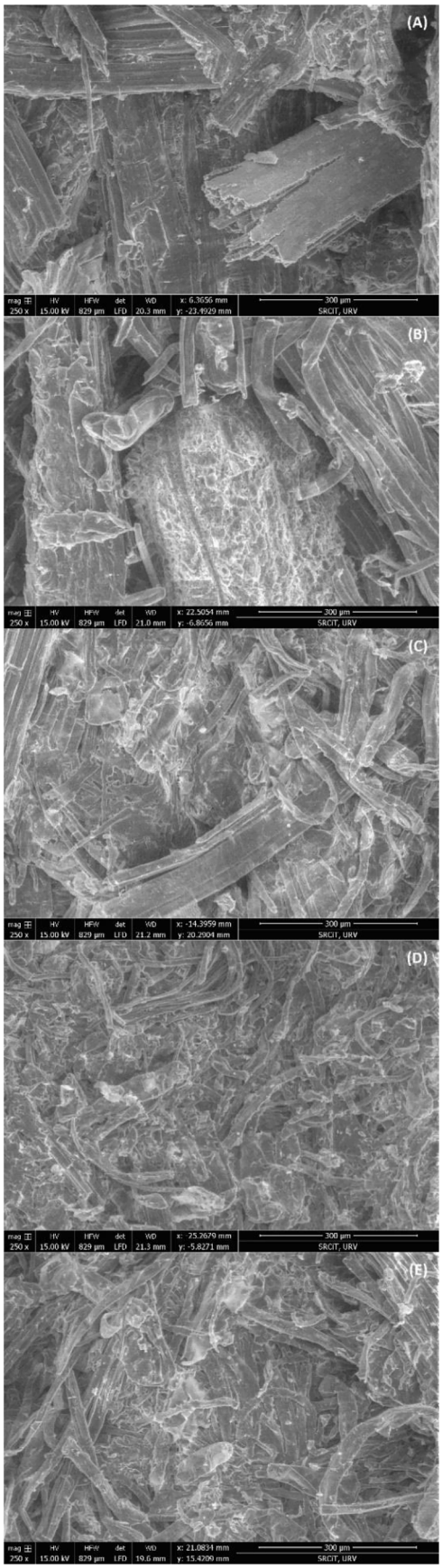

Fig. 9. Scanning Electron Microscope images of binderless fiberboards obtained by the exploded *Arundo donax* L. treated at Tr 187 °C (A), at 190 °C (B), at 195 °C (C), at 200 °C (D), and at 204 °C (E).

obtained for D series were very close and even better than commercial fiberboards. The addition of lignin has been associated with improved dimensional stability [53-55] and thus might be a solution for treatments C and E which fulfilled mechanical requirements but did not reach the required TS value.

All densities exceeded 900 kg/m^3, so all the binderless fiberboards can be considered high density fiberboards (Fig. 3). ANOVA results (Table 4) revealed the high dependence of density on R_0, since the p-value is much lower than 0.05. Having performed multiple comparisons (Table 5), it was observed that significant differences in the density values occurred between groups C-A, D-A, E-A, C-B, D-B, E-B, D-C, and E-C, while groups B-A and E-D did not have a statistically significant difference. As a result, we found that starting from a Tr of 195 °C, corresponding to the treatment C, the material is more defibrillated and thus more easily compactable. Thanks to this, the fiberboards obtained by treatments C, D, and E reached higher densities by using the same pressing pressure (Pp).

In Fig. 4a and Fig. 4b the boxplots of TS and WA respectively are reported. In both cases, best values were obtained for the pre-treatment carried out at 200 °C ($\log R_0 = 3.92$) which are 9.22% and 8.68%, respectively. As shown in Table 4, R0 was also statistically significant for dimensional stability and the multiple comparison (Table 5) revealed a statistically significant difference between groups C-A, D-A, E-A, C-B, D-B, and E-B. Again, the Tr of 195 °C represented the threshold beyond which properties improved significantly. From Figs. 4 and the data shown in Table 3, we also observed a worsening in fiberboard properties for treatment E, which could mean that the Tr of 200 °C of treatment D represented the optimum.

Fig. 5 and Fig. 6 show the boxplots of MOE and MOR results, respectively. The R_0 had a significant effect here as well (Table 4), while a multiple comparison (Table 5) showed that significant differences occurred between groups C-A, D-A, E-A, C-B, D-B, and E-B for MOE, and C-A, D-A, E-A, C-B, D-B, E-B, and D-C for MOR. The best results were obtained for Tr higher than 195 °C, i.e. treatment conditions C, D, and E, and particularly for treatment D.

As shown in Fig. 7, IB performed in a very similar manner to MOE and MOR, with values much higher for treatment conditions C, D, and E than A and B. Also, the p-value from ANOVA is the same as for the other properties (Table 4). The difference is in the multiple comparison where we found significant differences between all groups except for B-A, thus meaning that changes in Tr were much more significant for IB than the other properties.

3.2. Evaluation of morphological changes by SEM observation

Color change is a first indicator of chemical changes in the lignocellulosic structure of *Arundo donax* L. after steam explosion treatment. Fig. 8 shows the appearance of the fibers for each of the treatments considered in this study, before grinding. The color of the fibers became darker as the R_0 of the steam explosion treatment increased. This increase in darkness has been related to surface burning and the changes in extractives, lignin, and hemicellulose components [17,56], and it has been associated with the improvement in dimensional stability and mechanical properties [56,57]. Fig. 8 also shows the difference in the degree of defibrillation of the material: the treatments at the highest R_0 used led to a more defibrillated fiber and therefore more efficient hot pressing.

SEM observations supported the above statements. In Fig. 9 the SEM images of the binderless fiberboards obtained by the exploded *Arundo donax* L. at the different R_0 are compared. The increase in density was also apparent in fiberboard microstructure which is due to the effect of R_0 of steam explosion, as all fiberboards were hot pressed under the same conditions. In Fig. 9 (A) and Fig. 9 (B), which correspond to steam explosion at 187 °C and 190 °C, the fibers are almost intact. Fig. 9 (C) shows that the degree of defibrillation started to increase at a Tr of 195 °C, while Fig. 9 (D) and Fig. 9 (E) show a completely different

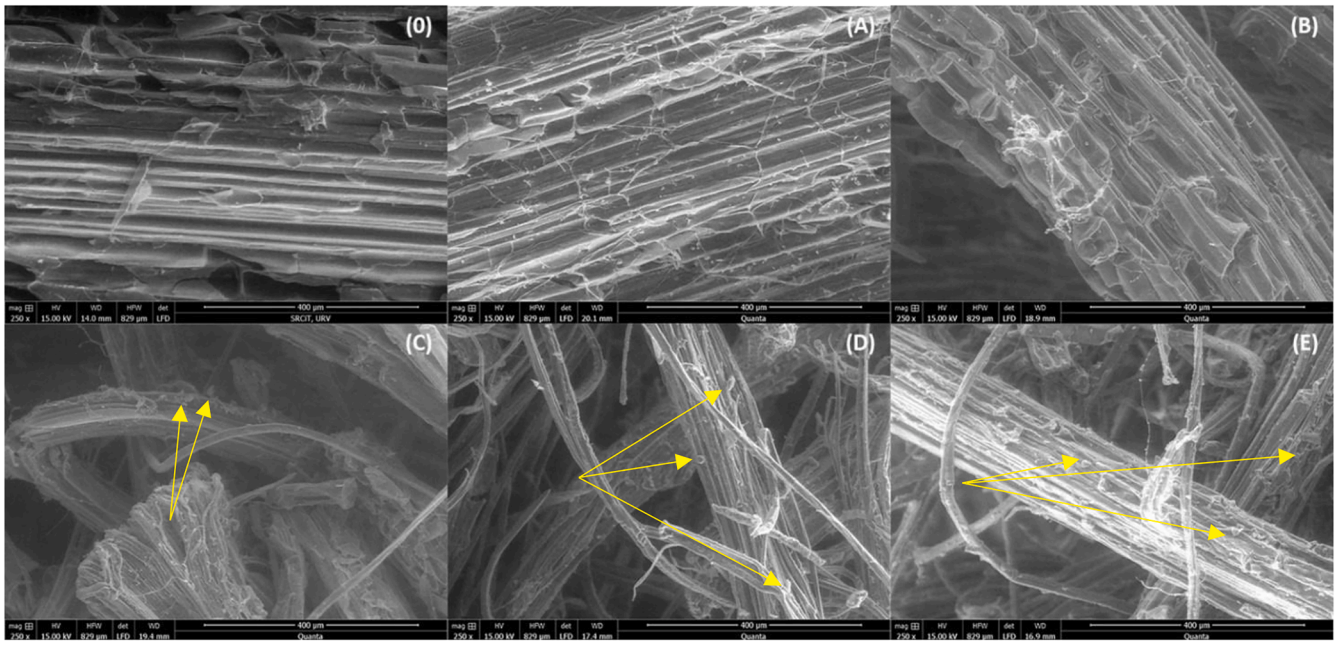

Fig. 10. Scanning Electon Microscope images of raw material (0), material treated at Tr 187 °C (A), at 190 °C (B), at 195 °C (C), at 200 °C (D), and at 204 °C (E).

morphology of exploded and hot pressed reeds.

In order to further explain this evidence, Fig. 10 shows SEM images of exploded giant reed at different R_0 before being ground and pressed to form fiberboards. Comparing the low R_0 treatment in Fig. 10 (A) and Fig. 10 (B) with raw material in Fig. 10 (0), no major differences were observed other than small fractures in the fiber surface, but the fibers appeared mostly unbroken. On the other hand, by increasing the Tr above 195 °C, long and thinner fibers were obtained (Fig. 10 (C), (D), (E)), as observed in other studies also [58]. The pre-treatment enlarged the contact area between fibers, thus the formation of hydrogen bonds during hot pressing was enhanced. Some studies [58] associated the decrease on MOR to the amorphous substance deposited on the fiber surface, consisting of degrading hemicellulose and lignin. In our study, we observed the same amorphous matter but no decrease in MOR values. This may be due to the rinsing step after pre-treatment as it washed away the residues of hydrolyzed hemicelluloses which could play a major role in the enhancement of the properties of binderless fiberboards. Thus, the amorphous structure may be the lignin that was redistributed between fibers after steam explosion. Troncoso-Ortega et al. [59] indicated the formation of pseudo-lignin during steam explosion pre-treatment, and its homogenous relocation in the cell wall surface or in the form of droplets, the abundance of which depends on R_0. In Fig. 10 (C), Fig. 10 (D), and Fig. 10 (E), drops of lignin can be clearly identified on the fiber surface.

3.3. Evaluation of chemical changes by FT-IR spectra analysis

FT-IR spectra analysis was carried out, aiming at corroborating chemical changes that apparently took place during steam explosion. Fig. 11 (a1), (a2), and (b) show FT-IR spectra of raw and exploded material, and spectra of binderless fiberboards obtained by all the severities respectively. The spectra confirmed that the major chemical changes occurred at the Tr of 195 °C and above: the pre-treatments C, D, an E showed spectra much more similar to those obtained for fiberboards, i.e. after grinding, hot-pressing, and curing. The absorption assignments presented in this work were based on the literature values [4,12,16,58,60]. At the wavenumber 3415 cm^{-1} the characteristic peak of hydroxyl group was reached. Hydroxyl groups are related to the formation of hydrogen bonds which enhance the IB of binderless fiberboards. In Fig. 11 the hydroxyl group peak clearly improved by increasing R_0 until the Tr of 200 °C, while for Tr 204 °C a small decrease in absorbance was detected, thus explaining the decrease of IB and mechanical properties for treatment E. At the wavenumber 1740 cm^{-1} the C = O stretching vibration, related to hemicelluloses, was reached. Both in Fig. 11 (a1), (a2), and in Fig. 11 (b), the hemicelluloses peak tended to disappear as the Tr increased, due to the hydrolyzation of hemicelluloses. The band of wavenumbers between 1632 cm^{-1} and 1509 cm^{-1} was associated to the aromatic core of lignin, which became clearly stronger by increasing Tr. Finally, the peaks included in the band of wavenumbers 1110 cm^{-1} and 1030 cm^{-1} were related to the hydroxyl group of polysaccharides, i.e. cellulose and hemicellulose. The transmittance associated with this peak showed the same tendency of 3415 cm^{-1} peak: the peak became stronger as the Tr was increased to the Tr of 200 °C. Above this point, the peak weakened.

3.4. Evaluation of thermal stability of binderless fiberboards by TGA curves

TGA was carried out in order to define the degradation temperatures of chemical components of *Arundo donax* L. and to verify the benefits that pre-treatment may bring in term of thermal stability. Fig. 12 shows the TGA and dTGA curves of raw untreated *Arundo donax* L. Three degradation steps can be clearly identified in the curves, as confirmed by other similar studies on lignocellulosic materials [12,14,61,62]. The first degradation step occurred between 30 °C and 100 °C and corresponded to the evaporation of water and volatile compounds [14,61]. The mass loss detected in this step was about 6%. The second step could be associated at the degradation of hemicellulose which starts around 200 °C, while the third step corresponded to the degradation of cellulose and lignin which occurs in the range of 240–350 °C and 280–500 °C respectively [14,61,63]. The TGA curve in Fig. 12 shows that the degradation steps of pyrolyzed *Arundo donax* L. are the same as those found in literature for other lignocellulosic materials. Indeed, the major mass loss of the material occurred in the 210–380 °C range and can be related to the degradation of the main components of lignocellulosic material, i.e. cellulose, hemicellulose, and lignin.

Fig. 13 (a) and (b) shows TGA and dTGA curves of binderless fiberboards obtained by exploded *Arundo donax* L. Comparing the curves of the binderless fiberboards with the raw material, a slight shift to the right occurred as the R_0 of the treatment increased. This means a main

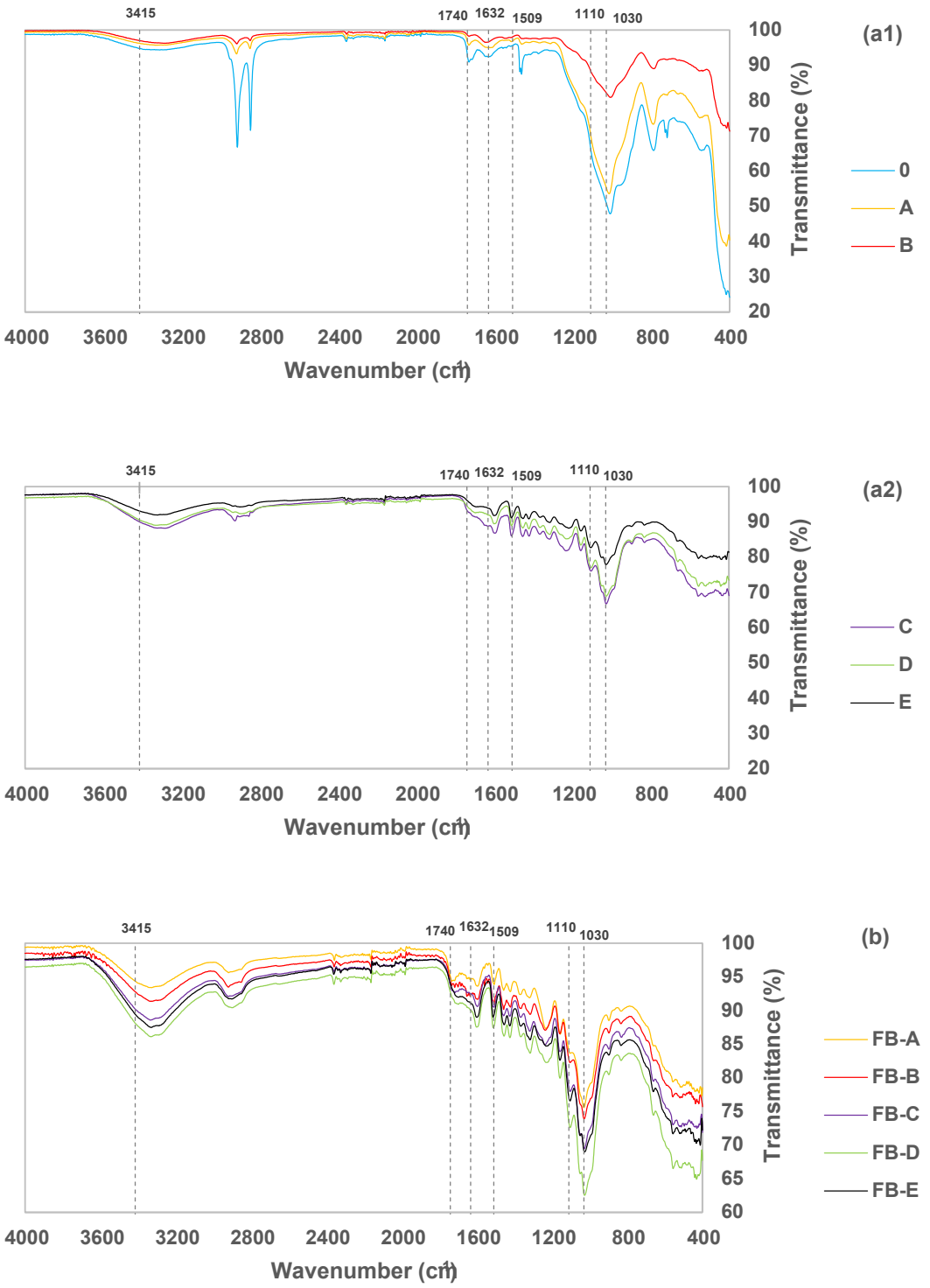

Fig. 11. FT-IR spectra of raw and exploded *Arundo donax* L. (a1) and (a2), and of binderless fiberboards (b).

role of steam explosion pre-treatment in thermal stability of each of the specimens. The maximum degradation peaks and the temperature range in which the main weight loss occurred for each of the specimens are shown in Table 6.

Char residues, or char yield (CY), are presented in Table 7. CY was obtained directly from the TGA test as the percentage of the residual mass remaining at the end of pyrolysis at a temperature above 800 °C. All samples showed a similar CY, although it seems that steam treatment produced a small improvement. Some studies [64,65] indicated that the ash content may cause operational problem such as slagging, deposit formation, equipment corrosion, and inorganic emissions, although it represents a major problem in biofuel production as it reduces the heating value [66]. Monti et al. [65] detected an ash content of 32 gkg^{-1} in *Arundo donax* L. stems. The percentage varies between 4.2 and 6.1% and decreases considerably if considering the pulp (Table 1). Several studies [64,67] are also available reporting the ash content in char obtained from *Arundo donax* L. pyrolysis. They reported a large variation (from 8.04% to 25.07%) depending on the temperature and the

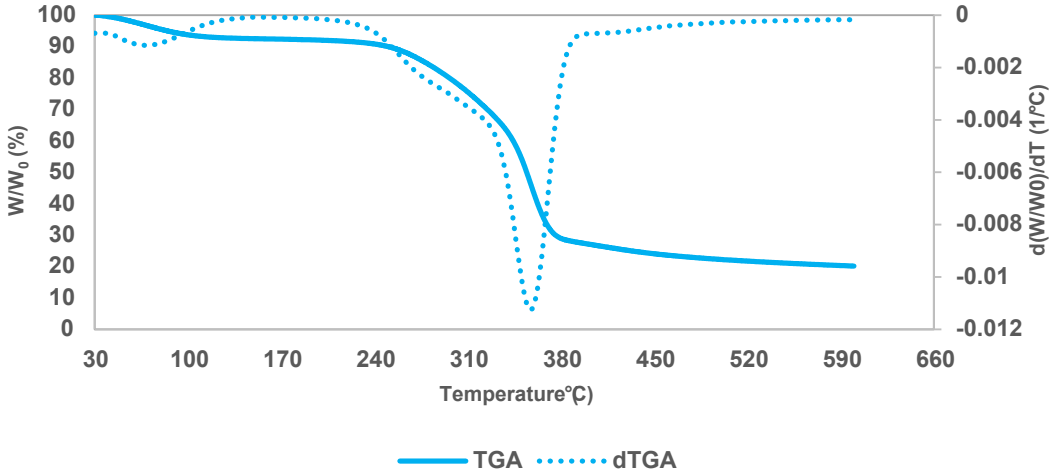

Fig. 12. TGA and dTGA curves of raw *Arundo donax* L.

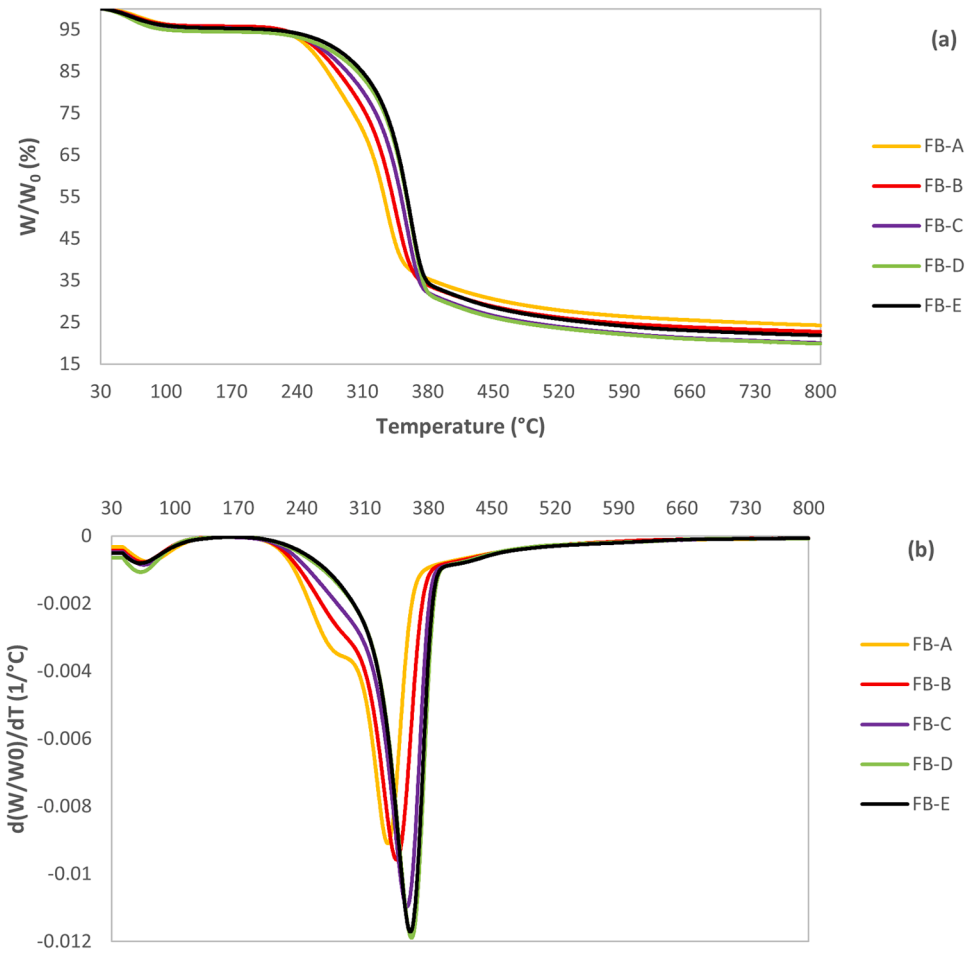

Fig. 13. TGA (a) and dTGA (b) of binderless fiberboards from steam exploded *Arundo donax L.*

composition of the biomass.

The CY is related to the limiting oxygen index (LOI) which permits to know the ability of a material to be flame-retardant and self-extinguishing [68]. The LOI is defined as the minimum O_2 concentration required to maintain combustion and can be calculated by the Van Krevelen and Hoftyzer equation as follows: [69]

$$LOI = 17.5 + 0.4CY$$

The minimum LOI for a material to be considered self-extinguishing is 28% and only the sample FB-A reached this value. However, the values of all the specimens were still very close and it seems that the pre-treatment produced an increase in CY and in the LOI when comparing samples to raw material. Moreover, although an increase in R_0 produced a decrease in CY, the CY increased again for treatment E, corresponding to the Tr of 204 °C. Further studies are needed to improve flame retardant ability.

Table 6
Temperature of maximum degradation peak and temperatures of main weight loss for raw material (0), and binderless fiberboards made by exploded *Arundo donax* L. at different severities.

Board type	Temperature of maximum degradation peak (°C)	Temperatures of main weight loss (°C)
0	400	230–380
FB-A	335	210–380
FB-B	345	210–380
FB-C	356	220–380
FB-D	361	220–380
FB-E	360	240–380

Table 7
Char Yield (CY) and Limiting Oxygen Index (LOI) of raw material (0) and of binderless fiberboards made by exploded *Arundo donax* L. at different severities.

Board type	CY (600 °C)	CY (800 °C)	LOI (600 °C)	LOI (800 °C)
	%	%	%	%
0	17.74	15.70	25.55	23.78
FB-A	26.27	24.25	28.01	27.20
FB-B	24.54	22.73	27.32	26.59
FB-C	22.15	20.05	26.36	25.52
FB-D	21.89	19.85	26.26	25.44
FB-E	23.89	21.86	27.06	26.25

4. Conclusions

The results presented in this study showed that major chemical and morphological changes occurred in steam exploded *Arundo donax* L. in a Tr range of 5 °C. A minimum Tr of 195 °C is necessary for *Arundo donax* L. binderless fiberboards to obtain physico-mechanical properties which fulfill the requirements. The best values were obtained with a Tr of 200 °C, while at 204 °C the physical and mechanical properties began to deteriorate, indicating that a further increase in the pre-treatment temperature may lead to a further deterioration of properties. For the Tr of 200 °C the mean results were 4514 MPa for MOE, 34.51 MPa for MOR, 4.125 MPa for IB, 8.68% for 24 h TS, and 9.22 for 24 h WA, which are comparable to commercial fiberboards properties.

SEM images showed the increase in the degree of defibrillation of the *Arundo donax* L. as the Tr increased, thus obtaining a pulp that can easily be pressed into fiberboards. This is also due to the redistribution of the lignin between the fibers, which was triggered from Tr 195 °C, and this enhanced the bonding of the fibers during hot pressing.

FT-IR spectra showed a correlation between the hydroxyl group and the decrease in IB and mechanical properties for Tr 204 °C. The hydroxyl group was related to the formation of hydrogen bonds between fibers which enhances the bonding between them. Changes in the *Arundo donax* L. structure were observed: above the Tr of 195 °C a spectra of exploded material very similar to the hot-pressed fiberboards were observed, while for lower Tr no appreciable changes compared to the raw material were remarked. This may mean that pre-treatment plays a greater role in activating fiber bonding than hot-pressing and curing. Therefore, by finding the Tr that activates the changes observed in this study, the same properties might be achieved with lower Pp and Tc or tc.

TGA curves showed the increase in thermal stability of the samples as the Tr increased, up to the Tr of 200 °C. This can be correlated to the similarity of the spectra of the material exploded at 195 °C, 200 °C, and 204 °C and the respective panels.

Finally, some considerations were drawn about CY and LOI which shows the ability of a material to be flame-retardant and self-extinguishing. Although most of the specimens did not reach the minimum LOI to be considered flame-retardant (28%), the values obtained were very close and improved thanks to the pre-treatment. Further studies are needed on this point to improve this ability.

Declaration of Competing Interest

The authors declare that they have no known competing financial interests or personal relationships that could have appeared to influence the work reported in this paper.

Acknowledgments

The authors wish to acknowledge the “Universitat Rovira i Virgili” (URV) for providing the research infrastructure and research support through a PhD scholarship. The authors would also like to thank the Generalitat de Catalunya (2017-SGR-77) for the financial support.

References

[1] A. Mahieu, A. Vivet, C. Poilane, N. Leblanc, Performance of particleboards based on annual plant byproducts bound with bio-adhesives, Int. J. Adhes. Adhes. 107 (2021), 102847, https://doi.org/10.1016/j.ijadhadh.2021.102847.
[2] F. Vitrone, D. Ramos, F. Ferrando, J. Salvadó, Binderless fiberboards for sustainable construction. Materials, production methods and applications, J. Build. Eng. 44 (2021), 102625, https://doi.org/10.1016/j.jobe.2021.102625.
[3] C.M. Sala, E. Robles, G. Kowaluk, Influence of the addition of spruce fibers to industrial-type high-density fiberboards produced with recycled fibers, Waste Biomass Valoriz. 1 (2020) 3, https://doi.org/10.1007/s12649-020-01250-8.
[4] J. Domínguez-Robles, Q. Tarrés, M. Alcalà, N.-E. el Mansouri, A. Rodríguez, P. Mutjé, M. Delgado-Aguilar, Development of high-performance binderless fiberboards from wheat straw residue, Construct. Build. Mater. 232 (2020), https://doi.org/10.1016/j.conbuildmat.2019.117247.
[5] T. Puspaningrum, Y.H. Haris, I. Sailah, M. Yani, N.S. Indrasti, Physical and mechanical properties of binderless medium density fiberboard (MDF) from coconut fiber, in, IOP Conf. Series: Earth Environ. Sci. 472 (1) (2020) 012011, https://doi.org/10.1088/1755-1315/472/1/012011.
[6] M. Ferrandez-Villena, A. Ferrandez-Garcia, T. Garcia-Ortuño, C.E. Ferrandez-Garcia, M.T.F. Garcia, Properties of wood particleboards containing giant reed (Arundo donax L.) particles, Sustainability. 12 (2020) 10469, https://doi.org/10.3390/su122410469.
[7] B. Shu, Q. Ren, L. Hong, Z. Xiao, X. Lu, W. Wang, J. Yu, N. Fu, Y. Gu, J. Zheng, Effect of steam explosion technology main parameters on moso bamboo and poplar fiber, Journal of Renewable Materials. 9 (2021) 585–597. 10.32604/jrm.2021.012932.
[8] E.H. Mejía, G.C. Quintana, B.O. Ogunsile, Development of binderless fiberboards from steamexploded and oxidized oil palm wastes, BioResources. 9 (2014) 2922–2936. 10.15376/biores.9.2.2922-2936.
[9] C.I.K. Diop, M. Tajvidi, M.A. Bilodeau, D.W. Bousfield, J.F. Hunt, Isolation of lignocellulose nanofibrils (LCNF) and application as adhesive replacement in wood composites: example of fiberboard, Cellulose 24 (7) (2017) 3037–3050, https://doi.org/10.1007/s10570-017-1320-z.
[10] M.C. Wong, S.I.S. Hendrikse, P.C. Sherrell, A. v. Ellis,, Grapevine waste in sustainable hybrid particleboard production, Waste Manage. 118 (2020) 501–509, https://doi.org/10.1016/j.wasman.2020.09.007.
[11] P. Hýsková, Š. Hýsek, O. Schönfelder, P. Šedivka, M. Lexa, V. Jarský, Utilization of agricultural rests: Straw-based composite panels made from enzymatic modified wheat and rapeseed straw, Ind. Crops Prod. 144 (2020), https://doi.org/10.1016/j.indcrop.2019.112067.
[12] C.P. Araújo Junior, C.A.C. Coaquira, A.L.A. Mattos, M.d.S.M. de Souza Filho, J.P.d. A. Feitosa, J.P.S.d. Morais, M. de Freitas Rosa, Binderless fiberboards made from unripe coconut husks, Waste Biomass Valoriz. 9 (11) (2018) 2245–2254, https://doi.org/10.1007/s12649-017-9979-9.
[13] E. Uitterhaegen, L. Labonne, O. Merah, T. Talou, S. Ballas, T. Véronèse, P. Evon, Impact of thermomechanical fiber pre-treatment using twin-screw extrusion on the production and properties of renewable binderless coriander fiberboards, Int. J. Mol. Sci. 18 (2017), https://doi.org/10.3390/ijms18071539.
[14] Z. A, M. T, W.-S.-M. Wmy, Mechanical, physical and thermal properties of rattan fibre-based binderless board, JTFS 29 (4) (2017) 485–492.
[15] A. Wechsler, M. Zaharia, A. Crosky, H. Jones, M. Ramírez, A. Ballerini, M. Nuñez, V. Sahajwalla, Macadamia (Macadamia integrifolia) shell and castor (Rícinos communis) oil based sustainable particleboard: A comparison of its properties with conventional wood based particleboard, Mater. Des. 50 (2013) 117–123, https://doi.org/10.1016/j.matdes.2013.03.008.
[16] S. Nonaka, K. Umemura, S. Kawai, Characterization of bagasse binderless particleboard manufactured in high-temperature range, J. Wood Sci. 59 (1) (2013) 50–56, https://doi.org/10.1007/s10086-012-1302-6.
[17] J.F. Hidalgo-Cordero, T. García-Ortuño, J. García-Navarro, Comparison of binderless boards produced with different tissues of totora (Schoenoplectus californicus (C.A. Mey) Soják) stems, J. Build. Eng. 27 (2020), https://doi.org/10.1016/j.jobe.2019.100961.
[18] J. Domínguez-Robles, Q. Tarrés, M. Delgado-Aguilar, A. Rodríguez, F.X. Espinach, P. Mutjé, Approaching a new generation of fiberboards taking advantage of self lignin as green adhesive, Int. J. Biol. Macromol. 108 (2018) 927–935, https://doi.org/10.1016/j.ijbiomac.2017.11.005.

[19] Z. Yang, W. Song, Y. Cao, C. Wang, X. Hu, Y. Yang, S. Zhang, The effect of laccase pretreatment conditions on the mechanical properties of binderless fiberboards with wheat straw, Bioresources. 12 (2017) 3707–3719.
[20] D. Theng, G. Arbat, M. Delgado-Aguilar, B. Ngo, L. Labonne, P. Mutjé, P. Evon, Production of fiberboard from rice straw thermomechanical extrudates by thermopressing: influence of fiber morphology, water and lignin content, Eur. J. Wood Wood Prod. 77 (1) (2019) 15–32, https://doi.org/10.1007/s00107-018-1358-0.
[21] Y. Kurokochi, M. Sato, Properties of binderless board made from rice straw: The morphological effect of particles, Ind. Crops Prod. 69 (2015) 55–59, https://doi.org/10.1016/j.indcrop.2015.01.044.
[22] M. Ferrandez-Villena, C.E. Ferrandez-Garcia, T.G. Ortuño, A. Ferrandez-Garcia, M. T. Ferrandez-Garcia, Study of the utilisation of almond residues for low-cost panels, Agronomy. 9 (2019), https://doi.org/10.3390/agronomy9120811.
[23] D. Battegazzore, J. Alongi, D. Duraccio, A. Frache, All natural high-density fiber- and particleboards from hemp fibers or rice husk particles, J. Polym. Environ. 26 (4) (2018) 1652–1660, https://doi.org/10.1007/s10924-017-1071-9.
[24] D. Theng, N.-E. el Mansouri, G. Arbat, B. Ngo, M. Delgado-Aguilar, M. Àngels Pèlach, P. Fullana-I-Palmer, P. Mutjé, Fibreboards made from corn stalk thermomechanical pulp and kraft lignin as a green adhesive, BioResources. 12 (2017).
[25] L. Corno, R. Pilu, F. Adani, G. Ricicla, Arundo donax L.: A non-food crop for bioenergy and bio-compound production, Biothechnol. Adv. 32 (2014) 1535–1549, https://doi.org/10.1016/j.biotechadv.2014.10.006.
[26] C.F. Lemons e Silva, M.A. Schirmer, R.N. Maeda, C.A. Barcelos, N. Pereira, Potential of giant reed (Arundo donax L.) for second generation ethanol production, Electron. J. Biotechnol. 18 (1) (2015) 10–15, https://doi.org/10.1016/j.ejbt.2014.11.002.
[27] M. Carnevale, L. Longo, F. Gallucci, E. Santangelo, Influence of the harvest time and the airflow rate on the characteristics of the Arundo biochar produced in a pilot updraft reactor, Biomass Convers. Biorefin. (2021), https://doi.org/10.1007/s13399-020-01241-8.
[28] W. Zegada-Lizarazu, S. Salvi, A. Monti, Assessment of mutagenized giant reed clones for yield, drought resistance and biomass quality, Biomass Bioenergy 134 (2020), 105501, https://doi.org/10.1016/j.biombioe.2020.105501.
[29] L.G. Angelini, L. Ceccarini, E. Bonari, Biomass yield and energy balance of giant reed (Arundo donax L.) cropped in central Italy as related to different management practices, Europ. J. Agronomy. 22 (4) (2005) 375–389, https://doi.org/10.1016/j.eja.2004.05.004.
[30] E. Alexopoulou, F. Zanetti, D. Scordia, W. Zegada-Lizarazu, M. Christou, G. Testa, S.L. Cosentino, A. Monti, Long-Term Yields of Switchgrass, Giant Reed, and Miscanthus in the Mediterranean Basin, (n.d.). 10.1007/s12155-015-9687-x.
[31] A. Jámbor, Á. Török, The economics of Arundo donax-A systematic literature review, Sustainability (Switzerland). 11 (2019), https://doi.org/10.3390/su11154225.
[32] F.W. Croon, Saving reed lands by giving economic value to reed, Mires and Peat. 13 (2013) 1–13. http://www.mires-and-peat.net/,ISSN1819-754X (accessed October 4, 2021).
[33] M. Ferrandez-Villena, C.E. Ferrandez-Garcia, T. Garcia-Ortuño, A. Ferrandez-Garcia, M.T. Ferrandez-Garcia, The influence of processing and particle size on binderless particleboards made from Arundo donax L. Rhizome, Polymers 12 (2020), https://doi.org/10.3390/polym12030696.
[34] M. Hardesty-Moore, D. Orr, D.J. McCauley, Invasive plant Arundo donax alters habitat use by carnivores, Biol. Invasions 22 (6) (2020) 1983–1995, https://doi.org/10.1007/s10530-020-02234-4.
[35] P.P. Dell'omo, V.A. Spena, Mechanical pretreatment of lignocellulosic biomass to improve biogas production: Comparison of results for giant reed and wheat straw, Energy. 203 (2020) 117798-undefined. 10.1016/j.energy.2020.117798.
[36] I. de Bari, F. Liuzzi, A. Ambrico, M. Trupo, Arundo donax Refining to second generation bioethanol and furfural, Processes 8 (2020) 1591, https://doi.org/10.3390/pr8121591.
[37] A.A. Shatalov, H. Pereira, Papermaking fibers from giant reed (Arundo donax L.) by advanced ecologically friendly pulping and bleaching technologies, BioResources 1 (2006) 45–61. https://www.researchgate.net/publication/26460087.
[38] E. Ukshini, J.J.J. Dirckx, Longitudinal and transversal elasticity of natural and artificial materials for musical instrument reeds, Materials 13 (2020) 1–13, https://doi.org/10.3390/ma13204566.
[39] A. Ferrarini, A. Fracasso, G. Spini, F. Fornasier, E. Taskin, M.C. Fontanella, G. M. Beone, S. Amaducci, E. Puglisi, Bioaugmented phytoremediation of metal-contaminated soils and sediments by hemp and giant reed, Front. Microbiol. 12 (2021), https://doi.org/10.3389/fmicb.2021.645893.
[40] D. Ramos, J. Salvadó, F. Ferrando, Arundo donax boards, 2017.
[41] D. Ramos, F. Ferrando, X. Farriol, J. Salvadó, Optimization of the production factors of boards obtained from Arundo Donax L. Fibers without added adhesives, Molecules 25 (2020), https://doi.org/10.3390/molecules25071660.
[42] D. Ramos, N.E. el Mansouri, F. Ferrando, J. Salvadó, All-lignocellulosic fiberboard from steam exploded Arundo donax L, Molecules 23 (2018), https://doi.org/10.3390/molecules23092088.
[43] L. Molari, F.S. Coppolino, J.J. García, Arundo donax: A widespread plant with great potential as sustainable structural material, Construct. Build. Mater. 268 (2021), https://doi.org/10.1016/j.conbuildmat.2020.121143, 121143-undefined.
[44] M.T. Ferrandez-Garcia, C.E. Ferrandez-Garcia, T. Garcia-Ortuño, A. Ferrandez-Garcia, M. Ferrandez-Villena, Experimental evaluation of a new giant reed (Arundo donax L.) composite using citric acid as a natural binder, Agronomy. 9 (2019), https://doi.org/10.3390/agronomy9120882.
[45] M. Nasir, D.P. Khali, M. Jawaid, P.M. Tahir, R. Siakeng, M. Asim, T.A. Khan, Recent development in binderless fiber-board fabrication from agricultural residues: A review, Constr. Build. Mater. 211 (2019) 502–516, https://doi.org/10.1016/j.conbuildmat.2019.03.279.
[46] W.G. Glasser, R.S. Wright, Steam-assisted biomass fractionation. II. Fractionation behavior of various biomass resources, (n.d.).
[47] H. Luo, H. Zhang, X. Lu, Manufacture of binderless fiberboard made from bamboo processing residues by steam explosion pretreatment, Wood Res. 59 (2014) 861–870. https://www.researchgate.net/publication/279098113.
[48] Y. Kurokochi, M. Sato, Steam treatment to enhance rice straw binderless board focusing hemicellulose and cellulose decomposition products, J. Wood Sci. 66 (2020) 1–8, https://doi.org/10.1186/s10086-020-1855-8.
[49] G. Quintana, J. Veí Asquez, S. Betancourt, P. Gã Ń An, Binderless fiberboard from steam exploded banana bunch, Ind. Crops Prod. 29 (2008) 60–66, https://doi.org/10.1016/j.indcrop.2008.04.007.
[50] M.T. Ferrandez-García, A. Ferrandez-Garcia, T. Garcia-Ortuño, C.E. Ferrandez-Garcia, M. Ferrandez-Villena, Assessment of the physical, mechanical and acoustic properties of Arundo donax L. biomass in low pressure and temperature particleboards, Polymers 12 (2020), https://doi.org/10.3390/POLYM12061361.
[51] Fractionation of lignocellulosics by steam-aqueous pretreatments, Philosophical Transactions of the Royal Society of London. Series A, Mathematical and Physical Sciences. 321 (1987) 523–536. 10.1098/rsta.1987.0029.
[52] F. Vitrone, D. Ramos, F. Ferrando, J. Salvadó, Binderless fiberboards for sustainable construction. Materials, production methods and applications, J. Build. Eng. 44 (2021), https://doi.org/10.1016/j.jobe.2021.102625.
[53] M.N. Anglès, F. Ferrando, X. Farriol, J. Salvadó, Suitability of steam exploded residual softwood for the production of binderless panels. Effect of the pre-treatment severity and lignin addition, Biomass Bioenergy 21 (3) (2001) 211–224.
[54] C. Mancera, N.-E. El Mansouri, M.A. Pelach, F. Francesc, J. Salvadó, Feasibility of incorporating treated lignins in fiberboards made from agricultural waste, Waste Manage. 32 (10) (2012) 1962–1967, https://doi.org/10.1016/j.wasman.2012.05.019.
[55] D. Theng, N.-E. el Mansouri, G. Arbat, B. Ngo, M. Delgado-Aguilar, M. Àngels Pèlach, P. Fullana-I-Palmer, P. Mutjé, Fibreboards Made from Corn Stalk Thermomechanical Pulp and Kraft Lignin as Green Adhesive, BioResources. 12 (2017).
[56] V.M. Tuong, J. Li, Effect of heat treatment on the change in color and dimensional stability of acacia hybrid wood, 2010.
[57] P. Bekhta, P. Niemz, Effect of high temperature on the change in color, dimensional stability and mechanical properties of spruce wood, Holzforschung 57 (2003) 539–546, https://doi.org/10.1515/HF.2003.080.
[58] B. Shu, Q. Ren, Q. He, Z. Ju, T. Zhan, Z. Chen, X. Lu, Study on mixed biomass binderless composite based on simulated wood, Wood Res. 64 (2019) 1023–1034.
[59] E. Troncoso-Ortega, R.D.P. Castillo, P. Reyes-Contreras, P. Castaño-Rivera, R. Teixeira Mendonça, N. Schiappacasse, C. Parra, Effects on lignin redistribution in eucalyptus globulus fibres pre-treated by steam explosion: A microscale study to cellulose accessibility, Biomolecules. 11 (2021), https://doi.org/10.3390/biom11040507.
[60] L.-P. Xiao, Z. Lin, W.-X. Peng, T.-Q. Yuan, F. Xu, N.-C. Li, Q.-S. Tao, H. Xiang, R.-C. Sun, Unraveling the structural characteristics of lignin in hydrothermal pretreated fibers and manufactured binderless boards from Eucalyptus grandis, Sustainable Chem. Processes 2 (2014) 9, https://doi.org/10.1186/2043-7129-2-9.
[61] M. Asadieraghi, W.M. Ashri, W. Daud, Characterization of lignocellulosic biomass thermal degradation and physiochemical structure: Effects of demineralization by diverse acid solutions, (2014). 10.1016/j.enconman.2014.03.007.
[62] Z. Chen, M. Hu, X. Zhu, D. Guo, S. Liu, Z. Hu, B. Xiao, J. Wang, M. Laghari, Characteristics and kinetic study on pyrolysis of five lignocellulosic biomass via thermogravimetric analysis, (2015). 10.1016/j.biortech.2015.05.062.
[63] J. Zhang, L. Feng, D. Wang, R. Zhang, G. Liu, G. Cheng, Thermogravimetric analysis of lignocellulosic biomass with ionic liquid pretreatment, (2013). 10.1016/j.biortech.2013.12.004.
[64] O. Oginni, K. Singh, Influence of high carbonization temperatures on key performance indicators of Arundo donax derived biochars, Biofuels (2021), https://doi.org/10.1080/17597269.2021.1948758.
[65] A. Monti, N. Di Virgilio, G. Venturi, Mineral composition and ash content of six major energy crops, Biomass Bioenergy 32 (3) (2008) 216–223, https://doi.org/10.1016/j.biombioe.2007.09.012.
[66] P. Giudicianni, S. Pindozzi, C.M. Grottola, F. Stanzione, S. Faugno, M. Fagnano, N. Fiorentino, R. Ragucci, Pyrolysis for exploitation of biomasses selected for soil phytoremediation: Characterization of gaseous and solid products, Waste Manage. 61 (2017) 288–299, https://doi.org/10.1016/j.wasman.2017.01.031.
[67] J. Yang, X. Wang, B. Shen, Z. Hu, L. Xu, S. Yang, Lignin from energy plant (Arundo donax): Pyrolysis kinetics, mechanism and pathway evaluation, Renewable Energy 161 (2020) 963–971, https://doi.org/10.1016/j.renene.2020.08.024.
[68] F. Pereira Marques, A.K. Lima Soares, D. Lomonaco, L.M. Alexandre e Silva, S. Tédde Santaella, M. de Freitas Rosa, R. Carrhá Leitão, Steam explosion pretreatment improves acetic acid organosolv delignification of oil palm mesocarp fibers and sugarcane bagasse, Int. J. Biol. Macromol. 175 (2021) 304–312, https://doi.org/10.1016/j.ijbiomac.2021.01.174.
[69] T. Periyasamy, S.P. Asrafali, S. Muthusamy, S.-C. Kim, Replacing bisphenol-A with bisguaiacol-F to synthesize polybenzoxazines for a pollution-free environment †, New J. Chem. 40 (2016) 9313, https://doi.org/10.1039/c6nj02242a.